ISSN 0006-2979, Biochemistry (Moscow), 2009, Vol. 74, No. 11, pp. 1203-1210. © Pleiades Publishing, Ltd., 2009.
Published in Russian in Biokhimiya, 2009, Vol. 74, No. 11, pp. 1479-1487.
Originally published in Biochemistry (Moscow) On-Line Papers in Press, as Manuscript BM09-080, September 13, 2009.

Primary Processes of Charge Separation in Reaction Centers of YM210L/FM197Y and YM210L Mutants of *Rhodobacter sphaeroides*

A. G. Yakovlev[1]*, L. G. Vasilieva[2], A. Y. Shkuropatov[2], and V. A. Shuvalov[1,2]

[1]*Department of Photobiophysics, Belozersky Institute of Physico-Chemical Biology, Lomonosov Moscow State University, 119991 Moscow, Russia; fax: (495) 939-3181; E-mail: yakov@genebee.msu.su*
[2]*Institute of Basic Biological Problems, Russian Academy of Sciences, 142290 Pushchino, Moscow Region, Russia; fax: (496) 779-0532; E-mail: shuvalov@issp.serpukhov.su*

Received March 12, 2009
Revision received May 18, 2009

Abstract—Difference femtosecond absorption spectroscopy with 20-fsec temporal resolution was applied to study a primary stage of charge separation and transfer processes in reaction centers of YM210L and YM210L/FM197Y site-directed mutants of the purple bacterium *Rhodobacter sphaeroides* at 90 K. Photoexcitation was tuned to the absorption band of the primary electron donor P at 880 nm. Coherent oscillations in the kinetics of stimulated emission of P* excited state at 940 nm and of anion absorption of monomeric bacteriochlorophyll B_A^- at 1020 nm were monitored. The absence of tyrosine YM210 in RCs of both mutants leads to strong slowing of the primary reaction $P^* \rightarrow P^+B_A^-$ and to the absence of stabilization of separated charges in the state $P^+B_A^-$. Mutation FM197Y increases effective mass of an acetyl group of pyrrole ring I in the bacteriochlorophyll molecule P_B of the double mutant YM210L/FM197Y by a hydrogen bond with OH-TyrM197 group that leads to a decrease in the frequency of coherent nuclear motions from 150 cm^{-1} in the single mutant YM210L to ~100 cm^{-1} in the double mutant. Oscillations with 100-150 cm^{-1} frequencies in the dynamics of the P* stimulated emission and in the kinetics of the reversible formation of $P^+B_A^-$ state of both mutants reflect a motion of the P_B molecule relatively to P_A in the area of mutual overlapping of their pyrrole rings I. In the double mutant YM210L/FM197Y the oscillations in the P* emission band and the B_A^- absorption band are conserved within a shorter time ~0.5 psec (1.5 psec in the YM210L mutant), which may be a consequence of an increase in the number of nuclei forming a wave packet by adding a supplementary mass to the dimer P.

DOI: 10.1134/S0006297909110042

Key words: photosynthesis, charge separation, reaction center, wave packet, electron transfer

The reaction center (RC) of bacterial photosynthesis is a membrane-bound pigment–protein complex in which conversion of light energy into energy of chemical bonds occurs as a result of a sequence of electron transfer reactions. The 3-dimensional structures of RC crystals of the purple bacteria *Rhodopseudomonas* (*Blastochloris*) *viridis* and *Rhodobacter sphaeroides* have been obtained by X-ray structure analysis [1, 2]. The *Rba. sphaeroides* RC consists of three protein subunits (L, M, and H) and several cofactors noncovalently bound to the transmembrane part of the subunits. The cofactors form two space-symmetrical branches (A and B). Each of the branches includes a dimer P consisting of excitonically coupled molecules of bacteriochlorophyll (BChl) P_A and P_B and acting as a primary electron donor, monomeric BChl (B_A or B_B), bacteriopheophytin (BPheo) (H_A or H_B), and quinone (Q_A or Q_B). The RC also includes an atom of non-heme iron and a carotenoid molecule. In RCs of purple bacteria charge separation occurs in the A-branch only. Upon light excitation of P, an electron transits from lowest excited singlet state P* to B_A with a time constant of ~3 psec at room temperature. A charge-separated state

Abbreviations: ΔA, absorption changes (light minus dark); BChl, bacteriochlorophyll; B_A and B_B, monomeric BChl in A- and B-branch, respectively; BPheo, bacteriopheophytin; H_A and H_B, BPheo in A- and B-branch, respectively; P, primary electron donor, dimer BChl; P_A and P_B, BChl molecules forming P; Q_A and Q_B, primary and secondary quinone, respectively; RC, reaction center; *Rba.*, *Rhodobacter*; *Rps.*, *Rhodopseudomonas*.

* To whom correspondence should be addressed.

$P^+B_A^-$ is formed at this time. The electron is passed further to H_A within ~1 psec, which leads to the formation of the $P^+H_A^-$ state. The fact that the $P^+B_A^-$ state is depleted several times faster than it is populated leads to significant difficulties in experimental registration of it. The electron transits further from H_A^- to Q_A with a time constant of ~200 psec at room temperature with formation of the $P^+Q_A^-$ state. At cryogenic temperatures, all of the mentioned reactions are 2-3 times faster. The quantum yield of charge separation is close to unity at all temperatures (for reviews, see in [3-5]).

Optical spectroscopy with femtosecond time resolution gives a unique possibility to study the influence of nuclear motion on electron transfer reactions. In [6-9] oscillations were found for the first time in the kinetics of P* stimulated emission in purple bacteria RCs upon femtosecond excitation. Analogous oscillations were found in the kinetics of spontaneous fluorescence [10]. These oscillations are connected with a coherent motion of the nuclear wave packet on the P* potential energy surface [7, 8, 11]. Oscillations have also been observed in the kinetics of charge separated states $P^+B_A^-$ and $P^+H_A^-$ [12-17]. Modulation of the B_A^- absorption band at 1020 nm with a ~260 fsec period reflecting reversible electron transfer from P* to B_A was found in [13-16]. Coherent oscillations of the $P^+H_A^-$ state population in *Rba. sphaeroides* RCs were revealed in the H_A absorption band bleaching at 760 nm [15-17]. Femtosecond oscillations in the kinetics of the P* stimulated emission at 945 nm and of the B_A^- absorption at 1028 nm were found in *Chloroflexus aurantiacus* RCs at 90 K [18].

It was found that in *Rba. sphaeroides* RCs femtosecond oscillations in the kinetics of the $P^+B_A^-$ state development are in phase with femtosecond oscillations in the kinetics of the P* stimulated emission at 940 nm and in anti-phase with the analogous oscillations at 900 nm [13]. Fourier spectra of the oscillations in the kinetics of the P* emission at 940 nm and of the B_A^- absorption at 1020 nm contain a main frequency at ~130 cm^{-1} that has mostly vibrational nature [16]. Moreover, in the Fourier spectra of the oscillations in the kinetics at 1020 nm a narrow intense band at 32 cm^{-1} is present together with its overtones, which probably indicates a contribution of vibrational modes of crystallographic water HOH55 [16]. A vibrational mode at ~150 cm^{-1} is also present in the Fourier spectra of the P* emission of the mutant YM210L *Rba. sphaeroides*, in which the primary charge separation is strongly slowed by substitution of tyrosine M210 by leucine [18]. In this mutant the character of the oscillations in the kinetics of the P* emission at 940 nm and of the B_A^- absorption at 1020 nm shows a reversibility of electron transfer between P* and B_A and an absence of stabilization of separated charges in the $P^+B_A^-$ state. Thus, the 130-150 cm^{-1} mode reflects mainly the properties of electron donor P870 and is not connected with the electron transfer reactions. This allows its use for monitoring of the condition of the dimer P. In present work the oscillation mode at ~150 cm^{-1} is used to study the primary processes of charge separation in the single mutant YM210L and the double mutant YM210L/FM197Y of the purple bacterium *Rba. sphaeroides*. The first mutation simplifies the form of the oscillations in the P* stimulated emission band with the ~150 cm^{-1} frequency and makes easier their registration on the background of almost constant non-oscillatory part of the kinetics. The second mutation adds a hydrogen bond to the acetyl-carbonyl group of ring I in P_B that can influence the condition of the dimer P [19].

MATERIALS AND METHODS

Mutants YM210L and YM210L/FM197Y were obtained by introducing of the gene into Puf M encoding the M subunits of *Rba. sphaeroides* reaction center using bacterial strains and plasmids as described in [20]. Mutant RCs as well as native *Rba. sphaeroides* RCs were isolated by treatment of the membranes with LDAO followed by chromatography with DEAE-cellulose [21]. For room temperature measurements, RCs were suspended in the 10 mM Tris-HCl, pH 8.0, 0.1% Triton X-100 buffer (TT buffer). Low-temperature measurements at 90 K were done with samples containing 65% glycerol (v/v). The optical density of the samples was 0.5 at 860 nm at room temperature. To keep RCs in the state $PB_AH_AQ_A^-$, 5 mM sodium dithionite was added.

Femtosecond measurements of absorption changes (light minus dark) were carried out with a laser spectrometer built on the basis of a Tsunami Ti-sapphire femtosecond laser pumped by a Millennia garnet laser (both from Spectra Physics, USA). Femtosecond laser pulses were amplified in an 8-passed Ti-sapphire amplifier and were used for generation of a probing continuum in a mixture of ordinary and heavy water (1 : 1). A part of the femtosecond continuum of 40 nm width centered at 880 nm was used as the pump emission. A polychromator and an optical multichannel analyzer were used for the measurements of the absorption change spectra at different delays (described in detail in [13]). The operating frequency of the spectrometer was 15 Hz. The duration of the pump and probe pulse was 20 fsec. The delay between the pump and probe pulse was varied with an accuracy of 0.1 fsec. Temporal dispersion in the 940-1060 nm range was compressed to a value less than 30 fsec.

The bulk of difference absorption spectra measured at various delays in the range from –0.1 to 4 psec with a 30-fsec step was the primary data. Each spectrum was a result of an averaging of 4000-7000 measurements. The accuracy of absorption measurements was $(1\text{-}3)\cdot10^{-5}$ optical density units. Amplitudes of the spectral bands at 1020 and 940 nm were measured at their maxima. The kinetics of absorption changes (ΔA) at 1020 and 940 nm

were plotted on the basis of measured amplitudes of absorption or bleaching bands. Oscillatory components of the kinetics were found by subtraction of the curves approximated by polynomials from the experimental kinetics. The oscillatory parts of the kinetics were analyzed by Fourier transformation to obtain frequency spectra of the oscillations. The polynomial rather than exponential approximation of the kinetics is appropriate in studying the primary stages of electron transfer with a large contribution of adiabatic processes.

RESULTS

In the present work, we studied the femtosecond oscillations in the kinetics of the single mutant YM210L and the double mutant YM210L/FM197Y RCs from the purple bacterium *Rba. sphaeroides*, paying special attention to the effects caused by substitution of a phenylalanine residue by tyrosine residue in the M197 position. It was found earlier that tyrosine incorporated in the M197 position donates a hydrogen bond to the acetyl-carbonyl group of ring I in the P_B molecule, whereas the natural phenylalanine M197 does not create such bond [19]. However, the analogous hydrogen bond naturally takes place in wild type RCs of *Rps. viridis* [22], and the speed of the primary charge separation reaction in these RCs is greater than in *Rba. sphaeroides* RCs. One can assume that the additional hydrogen bond to BChl P_B will influence the vibrational modes activated by femtosecond photoexcitation of P (Fig. 1).

In Fig. 2 the difference (light minus dark) absorption spectra of the mutant YM210L and YM210L/FM197Y RCs of *Rba. sphaeroides* are shown in the 980-1050 nm range at some femtosecond delays with respect to the photoexcitation, measured at 90 K. At a wavelength shorter than 990 nm, the bleaching caused by the P* stimulated emission dominates in the spectra of both mutants. In the 1020 nm area, a weak but clearly distinct and reliably repeated absorption band ascribed to B_A^- anion is observed. The amplitude of this band changes in time periodically with appearance followed by almost disappearance, but its spectral position remains the same for the two mutants. The bulk of the difference spectra measured in the –0.1-to-4 psec delay range with a 30 fsec step was used to plot the kinetics of the P* emission at 940 nm and of the B_A^- absorption at 1020 nm that are shown in Fig. 3. The P* stimulated emission at 940 nm (Fig. 3a) of both mutants shows practically no decay within the whole studied range of delays 0-4 psec. For the YM210L mutant a characteristic time of the P* emission decay is 190 psec at 10 K [9]. For the YM210L/FM197Y mutant the midpoint potential of P/P^+ pair is 30 mV higher than for the YM210L mutant, which leads to further decreasing of the driving force of electron transfer reaction and can further slow the P* emission decay [23]. The kinetics of both mutants at 940 nm contains marked oscillations with approximately the same amplitude. In the kinetics of YM210L mutant at 940 nm, seven peaks of the oscillations with ~220 fsec period are distinguished and also marked oscillation decay is observed at delays later than 1.5 psec. The oscillations in the double mutant kinetics at 940 nm have a longer period and decay much faster – at delays longer than 0.5 psec. The kinetics of both mutants at 1020 nm (Fig. 3b) shows practically complete absence of the B_A^- absorption band at delays longer than 1.5 psec. This is in agreement with earlier obtained data for the YM210L mutant [18] and means a complete reversibility of electron transfer between P* and B_A, that is the absence of separated charge stabilization in the $P^+B_A^-$ state. At the delays less than 1.5 psec, expressed oscillations with a complex shape are observed in the kinetics of both mutants at 1020 nm. The amplitude of these oscillations in the double mutant is somewhat less than in the single

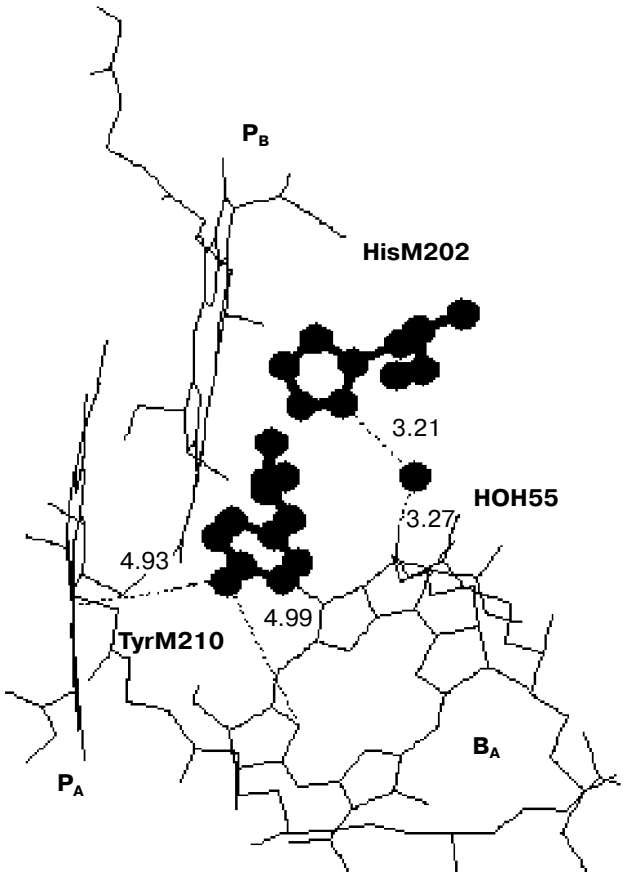

Fig. 1. Structure of dimer of bacteriochlorophylls P_A and P_B and of monomeric bacteriochlorophyll B_A of *Rba. sphaeroides* RCs (Brookhaven data bank, file 1AIJ). Histidine M202, liganding the Mg ion of P_B, is connected by a hydrogen bond to a H_2O molecule and further to the oxygen of the keto carbonyl group of ring V of B_A. The distance between the oxygen of TyrM210 (analogous to M208 in *Rps. viridis* RCs) and $P_A(B_A)$ is 4.93 (4.99) Å with maximal electron spin density on $P^+(B_A^-)$. Numbers show distances in Å.

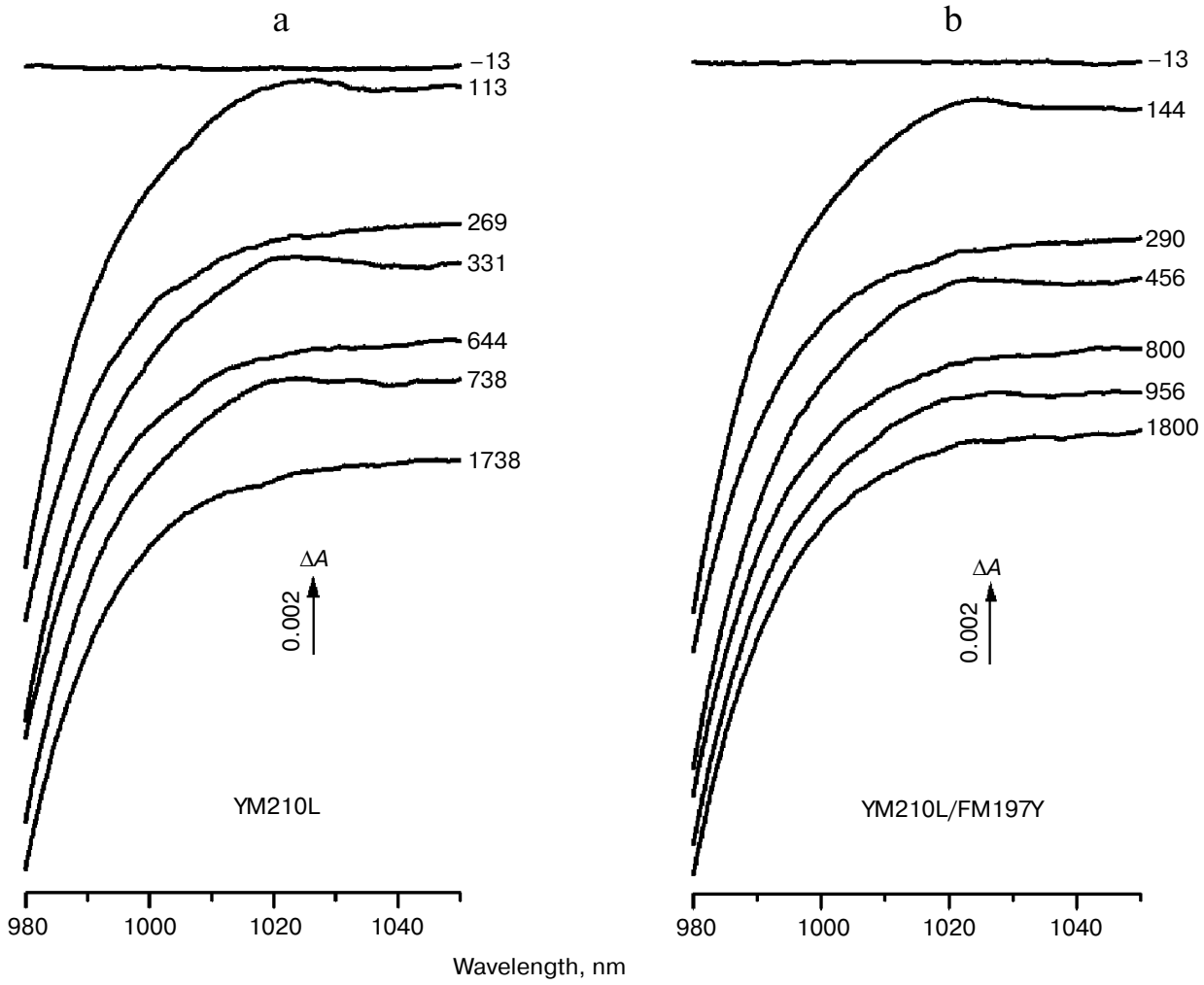

Fig. 2. Difference (light minus dark) absorption spectra of RCs of mutant YM210L (a) and YM210L/FM197Y (b) of *Rba. sphaeroides* in glycerol-TT buffer in the 980-1050 nm range, measured at various femtosecond delays at 90 K. The RCs were excited by 20 fsec pulses at 880 nm. Numbers show the measurement delay in femtoseconds. Spectra are shifted vertically for clearness.

mutant. Note that the oscillations in the kinetics at 940 and 1020 nm in RCs of both mutants are in phase with each other.

The Fourier spectrum at 940 nm of the YM210L mutant contains two main bands at 152 and 94 cm^{-1} and less intense bands at 121 and 66 cm^{-1} (Fig. 4a). The Fourier spectrum of the double mutant contains a broad band in the ~100 cm^{-1} area with maximums at 87 and 108 cm^{-1} (Fig. 4a). A ~10 cm^{-1} peak in the spectra of both mutants reflects a global asymmetry of the oscillation curves and probably does not have physical sense. The Fourier spectrum of the 1020 nm band oscillations of the YM210L mutant contains a dominant band at 33 cm^{-1} and less intense bands at 99 and 155 cm^{-1} (Fig. 4c). The last two bands are observed also in the Fourier spectra of this mutant at 940 nm (bands at 94 and 152 cm^{-1}, Fig. 4a) and most probably are of vibrational nature. The 33 cm^{-1} band might reflect a rotational motion of the water molecule HOH placed in the RC near P and B_A (Fig. 1) [18]. The Fourier spectrum of the oscillations in the absorption at 1020 nm in RCs of the double mutant (Fig. 4c) contains a broad band at ~100 cm^{-1} and a lower frequency band with maximums at 21 and 37 cm^{-1}. The band at ~100 cm^{-1} is observed in the Fourier spectrum of this mutant at 940 nm and also is probably of vibrational nature.

DISCUSSION

It is shown in the present work that the main band in the Fourier spectrum of the oscillations at 940 and 1020 nm is shifted from 150 cm^{-1} in the single mutant YM210L to ~100 cm^{-1} in the double mutant YM210L/FM197Y *Rba. sphaeroides* (Fig. 4). A frequency drop or a reduction of motion speed might be a conse-

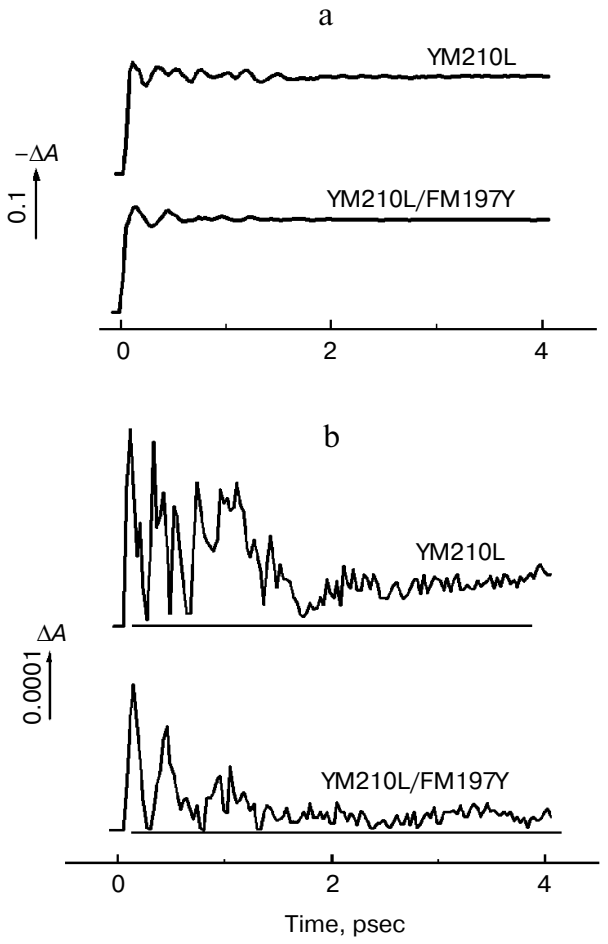

Fig. 3. Kinetics ΔA in RCs of mutant YM210L and YM210L/FM197Y of *Rba. sphaeroides* in glycerol-TT buffer at 90 K in the 940 nm band (P* stimulated emission) (a) and in the 1020 nm band (B_A^- absorption) (b). RCs were excited by 20 fsec pulses at 880 nm. The curves are shifted vertically for clearness.

quence of an increasing of the effective mass of some part of coordinately oscillated (because of femtosecond excitation) molecular groups because of addition of new groups via a hydrogen bond. As the increasing of the effective mass of the acetyl group of pyrrole ring I is supposed for the P_B molecule in the double mutant RCs due to creation of a hydrogen bond with the OH-TyrM197 group [19], then pyrrole ring I of the bacteriochlorophyll P_B probably participates in a nuclear motion induced by femtosecond photoexcitation of P at 880 nm. A similar decreasing of oscillation frequency was found in the kinetics of P* stimulated emission in RCs of mutant FM197H *Rba. sphaeroides* [7, 8, 17]. In this mutant a new hydrogen bond is created between the acetyl-carbonyl group of ring I in P_B and the incorporated new histidine M197 [22]. In the mutant HL168F, on the contrary, removing of the naturally existing hydrogen bond between the acetyl-carbonyl group of ring I in P_A and the natural histidine HL168 takes place. However, frequency increasing of the oscillations in the P* kinetics does not occur in this mutant [24]. This may indicates that pyrrole ring I of the P_A molecule is not fixed enough in the RC structure and is not involved in the nuclear motions activated by femtosecond excitation of P.

Thus, the femtosecond oscillations with 100-150 cm^{-1} frequencies in the kinetics of the P* stimulated emission and of the reversible population of $P^+B_A^-$ state probably reflect a motion of the P_B molecule relative to P_A in the area of mutual overlapping of its pyrrole rings I (Fig. 1). One of the spectral and functional consequences of this motion could be the formation of a molecular complex with charge transfer in the excited state by analogy to the well-known excimer and exciplex complexes that are formed between aromatic rings of excited dye molecules in solution [25]. These molecular dimers are formed in the dye excited states and have a parallel orientation of the conjugated electron systems with partial charge transfer between them. The excimer and exciplex formation is accompanied by a shift of the fluorescence spectrum to longer wavelengths in comparison with the spectra of monomeric dye molecules. Perhaps the formation of these excited dimers occurs between the two BChl molecules in the P dimer when ring I in P_B is maximally approaching ring I in P_A. In this case the appearance of the long-wavelength P* stimulated emission at 940 nm can be interpreted as a manifestation of the dynamic formation of an exciplex-like complex between the P_A and P_B molecules.

It was shown in the theoretical work [26] that in the P* excited state the charge distribution is characterized by a strong shift of the electron density from P_A to P_B in the proportion 0.76/0.24. This might mean that the motion of P_B nuclei with respect to P_A because of the formation of the nuclear wave packet is accompanied by the long-wavelength shift of the P* stimulated emission and the partial charge transfer from P_A to P_B with the creation of the $P_A^{\delta+}P_B^{\delta-}$ state. When the distance between pyrrole rings I in P_A and P_B is minimal, the shift of the electron density from P_A to P_B is maximal and the long-wavelength shift of the P* stimulated emission is maximal as well (up to 940 nm).

A formal similarity of the Fourier spectra of the kinetics at 940 and 1020 nm of the YM210L mutant and the similar low-frequency shift of these spectra in the double mutant YM210L/FM197Y indicates the activity of the low-frequency modes of the P* emission during the process of electron transfer from P* to B_A. The appearance of the P* stimulated emission at 940 nm is accompanied by the appearance of an electron at the B_A molecule (Fig. 4). This might mean that the formation of a component with $P_A^{\delta+}P_B^{\delta-}$ state character in the P* state leads to electron transfer from $P_B^{\delta-}$ to B_A. Perhaps this transfer occurs along a chain of polar groups N–Mg(P_B)–N–C–N(HisM202)–HOH–O=(B_A), connecting P_B and B_A (Fig. 1) [16].

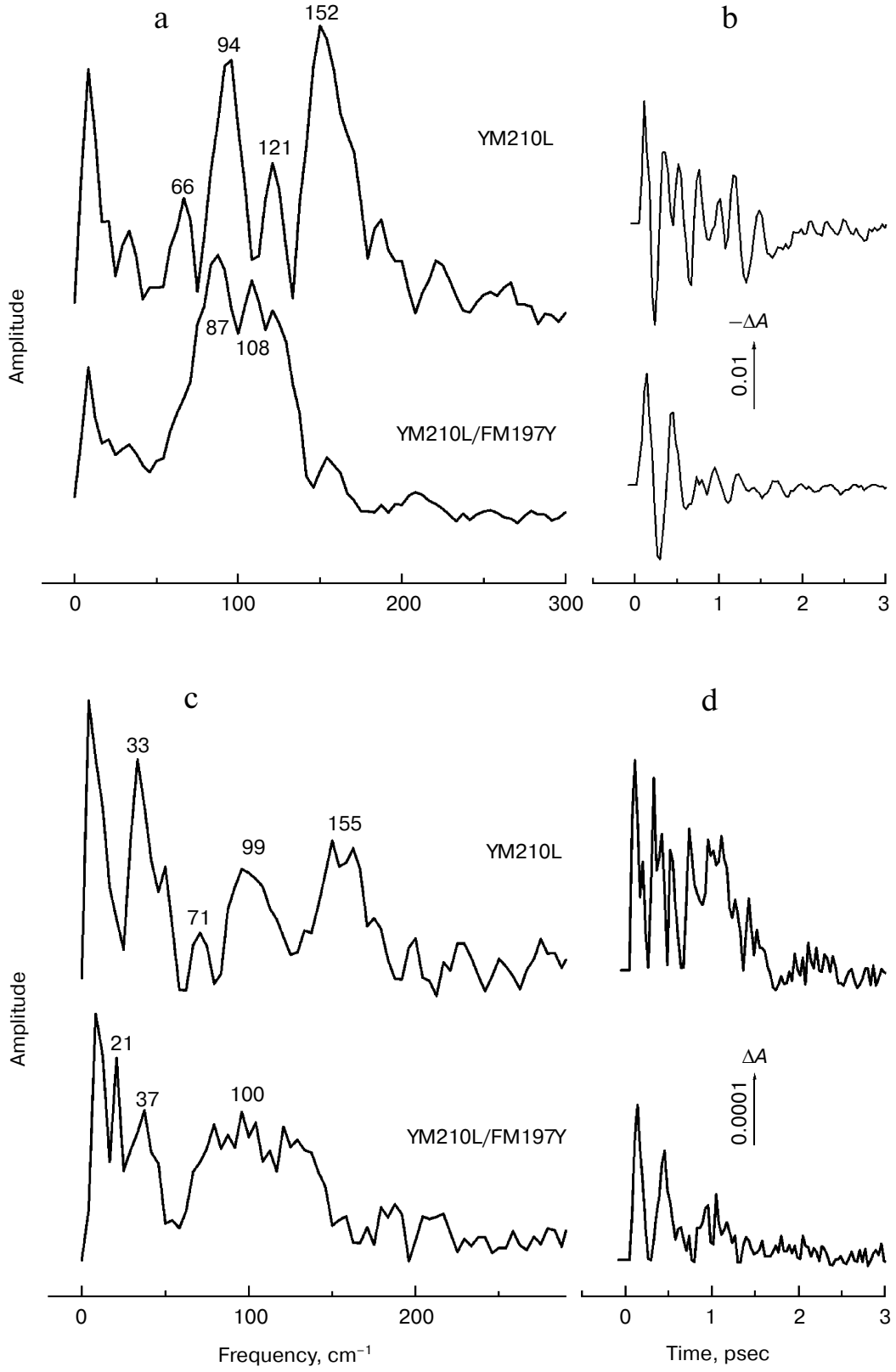

Fig. 4. Fourier spectra (a, c) of oscillatory components (b, d) of the kinetics ΔA for the 940 nm band (P* stimulated emission) (a, b) and for the 1020 nm band (B_A^- absorption) (c, d) in RCs of mutant YM210L and YM210L/FM197Y of *Rba. sphaeroides* in glycerol-TT buffer at 90 K. The RCs were excited by 20 fsec pulses at 880 nm. Numbers show position of band maximums in the Fourier spectra in cm^{-1}. The curves are shifted vertically for clearness.

A simplified scheme of potential energy levels illustrates a process of non-equilibrium conversion of the P* excited state into the charge separated states in RC (Fig. 5). A 20 fsec light excitation of P forms the nuclear wave packet on the potential energy surface of the lowest exciton state $\sqrt{½}\{|P_A^*P_B> + |P_AP_B^*>\} \equiv |+>$ with the emission at 895 nm (electron coupling between P_A and P_B has a negative energy ~600 cm^{-1}). The primary charge separation probably occurs inside the dimer P with creation of the $|P_A^{\delta+}P_B^{\delta-}>$ state. The potential energy surface of this state is shifted with respect to those for the |+> state, and consequently the emission from the $|P_A^{\delta+}P_B^{\delta-}>$ surface has a wavelength ~940 nm. In the intersection area, these surfaces are split because of the strong electron coupling. The electron coupling between P* and B_A (~30 cm^{-1}) splits the original surfaces (P* and $P^+B_A^-$) into upper and lower parts. For the effective electron transfer to B_A it is necessary that the $P^+B_A^-$ surface intersects with the $|P_A^{\delta+}P_B^{\delta-}>$ surface near the bottom of the later. When the nuclear wave packet with enough energy (~150 cm^{-1}) moves on the |+> surface it probably reaches the $P_A^{\delta+}P_B^{\delta-}$ surface and further the intersection of it with the $P^+B_A^-$ surface at the ~120 fsec delay. In this case, a portion of the $P_A^{\delta+}P_B^{\delta-}$ state is strongly increased, which accelerates the electron transfer to B_A. At the ~120 fsec delay the P* stimulated emission at 940 nm and B_A^- absorption band formation at 1020 nm occurs, which corresponds to the first maximum in the oscillations of the kinetics ΔA at 940 and 1020 nm (Figs. 3 and 4). Then the wave packet can be reflected back to the P* surface or partially move to the $P^+B_A^-$ surface.

A stabilization of separated charges in P^+ and B_A^- in native RCs can occur with participation of the OH-group of the tyrosine TyrM210 (TyrM208 in RCs *Rps. viridis*) (Fig. 1) [5, 18]. TyrM210 is at ~4.93 Å distance from the nearest C atom of ring IV in P_A when maximal electron spin density is on P^+, and at ~4.99 Å distance from the N atom of ring II in B_A when maximal electron spin density is on B_A^- [26]. The stabilization might occur due to a reorientation of surrounding molecular groups when the $P^+B_A^-$ state is formed. When the nuclear wave packet formed by photoexcitation reaches the intersection area of the potential surfaces of the P* and $P^+B_A^-$ states, its further evolution depends on additional changes of P and B_A surrounding nuclei positions. If changes that break system coherency are absent, then the wave packet will stay on the P* surface and will begin to move back. If such changes are present, then the oscillatory motions of the nuclear wave packet in the P* state can be suppressed. The necessary changes of such kind can occur in native RCs as a result of the reorientation of the polar group like $O^{\delta-}H^{\delta+}$ in TyrM210 (TyrM208 in *Rps. viridis*) (Fig. 1), which leads to significant suppression of the oscillations during a time interval of about 0.5 psec [16]. The absence of TyrM210 in the mutant YM210L conserves the oscillations in the P* emission band and in the B_A^- absorption band during considerably longer time interval ~1.5 psec after the P excitation (Fig. 4). This might mean that in native RCs the motion of $H^{\delta+}$ of the OH–TyrM210 group in the direction of B_A^- lowers the energy level of the $P^+B_A^-$ state with respect to P*, which leads to irreversible electron transfer to B_A and a fast dephasing of the coherent oscillations of the system. Calculations show that the energy of Coulomb interaction between the group $H^{\delta+}O^{\delta-}$–TyrM210 and B_A^- or P^+ can be estimated as 890 cm^{-1} [5, 18]. Experimental estimations of the energy difference of P* and $P^+B_A^-$ levels in the stabilized $P^+B_A^-$ state are 350-550 cm^{-1} [27]. Thus, the interaction energy is enough to stabilize an electron on B_A^- if $H^{\delta+}$ of the OH–TyrM210 group will be shifted towards B_A during charge separation. In the double mutant YM210L/FM197Y oscillations in the P* emission band and the B_A^- absorption band are conserved during shorter time ~0.5 psec (Fig. 4) than in the single mutant YM210L, which (in the absence of irreversible electron transfer) might be a consequence of an increasing of a number of nuclei forming the wave packet by adding a supplementary mass to the dimer P via the hydrogen bond with the OH–TyrM197 group.

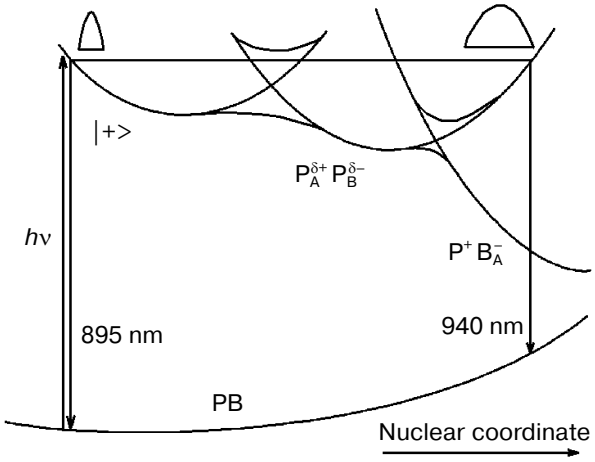

Fig. 5. Illustrative scheme of potential energy surfaces of the following states: ground (PB_A), locally excited (P^*B_A), charge separated ($P^+B_A^-$).

The authors thank T. I. Bolgarina and V. A. Shkuropatova for help in RCs sample preparation.

This work was done with financial support of the Russian Foundation for Basic Research (grant No. 08-04-00888) and the Russian Academy of Sciences (grant MCB).

REFERENCES

1. Deisenhofer, J., Epp, O., Miki, K., Huber, R., and Michel, H. (1984) *J. Mol. Biol.*, **180**, 385-398.

2. Allen, J. P., Feher, G., Yeates, T. O., Komiya, H., and Rees, D. C. (1987) *Proc. Natl. Acad. Sci. USA*, **84**, 5730-5734.
3. Kirmaier, C., and Holten, D. (1993) in *The Photosynthetic Reaction Center* (Deisenhofer, J., and Norris, J., eds.) Academic Press, San Diego, pp. 49-70.
4. Woodbury, N. W., and Allen, J. P. (1995) in *Anoxygenic Photosynthetic Bacteria* (Blankenship, R. E., Madigan, M. T., and Bauer, C. E., eds.) Kluwer Academic Publishers, Dordrecht, pp. 527-557.
5. Shuvalov, V. A., and Yakovlev, A. G. (2003) *FEBS Lett.*, **540**, 26-34.
6. Vos, M. H., Lambry, J.-C., Robles, S. J., Youvan, D. C., Breton, J., and Martin, J.-L. (1991) *Proc. Natl. Acad. Sci. USA*, **88**, 8885-8889.
7. Vos, M. H., Rappaport, F., Lambry, J.-C., Breton, J., and Martin, J.-L. (1993) *Nature*, **363**, 320-325.
8. Vos, M. H., Jones, M. R., Hunter, C. N., Breton, J., Lambry, J.-C., and Martin, J.-L. (1994) *Biochemistry*, **33**, 6750-6757.
9. Vos, M. H., Jones, M. R., Breton, J., Lambry, J.-C., and Martin, J.-L. (1996) *Biochemistry*, **35**, 2687-2692.
10. Stanley, R. J., and Boxer, S. G. (1995) *J. Phys. Chem.*, **99**, 859-863.
11. Sporlein, S., Zinth, W., and Wachtveitl, J. (1998) *J. Phys. Chem. B*, **102**, 7492-7496.
12. Streltsov, A. M., Vulto, S. I. E., Shkuropatov, A. Ya., Hoff, A. J., Aartsma, T. J., and Shuvalov, V. A. (1998) *J. Phys. Chem. B*, **102**, 7293-7298.
13. Yakovlev, A. G., Shkuropatov, A. Ya., and Shuvalov, V. A. (2000) *FEBS Lett.*, **466**, 209-212.
14. Yakovlev, A. G., and Shuvalov, V. A. (2000) *J. Chin. Chem. Soc.*, **47**, 709-714.
15. Yakovlev, A. G., Shkuropatov, A. Ya., and Shuvalov, V. A. (2002) *Biochemistry*, **41**, 2667-2674.
16. Yakovlev, A. G., Shkuropatov, A. Ya., and Shuvalov, V. A. (2002) *Biochemistry*, **41**, 14019-14027.
17. Vos, M. H., Rischel, C., Jones, M. R., and Martin, J.-L. (2000) *Biochemistry*, **39**, 8353-8361.
18. Yakovlev, A. G., Vasilieva, L. G., Shkuropatov, A. Ya., Bolgarina, T. I., Shkuropatova, V. A., and Shuvalov, V. A. (2003) *J. Phys. Chem. A*, **107**, 8330-8338.
19. Kuglstatter, A., Hellwig, P., Fritzsch, G., Wachtveitl, J., Oesterhelt, D., Mantele, W., and Michel, H. (1999) *FEBS Lett.*, **463**, 169-174.
20. Vasilieva, L. G., Bolgarina, T. I., Chatipov, R. A., Shkuropatov, A. Y., and Shuvalov, V. A. (2001) *Doklady RAN*, **376**, 826-829.
21. Shuvalov, V. A., Shkuropatov, A. Y., Kulakova, S. M., Ismailov, M. A., and Shkuropatova, V. A. (1986) *Biochim. Biophys. Acta*, **849**, 337-348.
22. Michel, H., Epp, O., and Deisenhofer, J. (1986) *EMBO J.*, **5**, 2445-2451.
23. Lin, X., Marchison, H. A., Nagarajan, V., Parson, W. W., Allen, J. P., and Williams, J. C. (1994) *Proc. Natl. Acad. Sci. USA*, **91**, 10265-10269.
24. Rischel, C., Spiedel, D., Ridge, J. P., Jones, M. R., Breton, J., Lambry, J.-L., Martin, J.-L., and Vos, M. H. (1998) *Proc. Natl. Acad. Sci. USA*, **95**, 12306-12311.
25. Beens, H., and Weller, A. (1975) in *Organic Molecular Photophysics* (Birks, J. B., ed.) Vol. 11, John Willey&Sons, London, pp. 159-215.
26. Plato, M., Lendzian, F., Lubitz, W., Trankle, E., and Mobius, K. (1988) in *The Photosynthetic Bacterial Reaction Center: Structure and Dynamics* (Breton, J., and Vermeglio, A., eds.) Plenum Press, N.Y.-London, pp. 379-388.
27. Shuvalov, V. A., and Yakovlev, A. G. (1998) *Membr. Cell Biol. (Moscow)*, **12**, 563-569.